

无机化学学报

2020年

第36卷

第1期

目次

论 文

- 硝酸活化三聚氰胺前驱体对 $g\text{-C}_3\text{N}_4$ 结构和可见光催化性能的影响
..... 叶仕雄 舒庆(1)
- 全固态 Z-型 $\text{CdS}/\text{Au}/\text{Bi}_2\text{MoO}_6$ 异质结的构筑及其光催化性能
..... 郭莉 赵强 张越诚 张媛媛 韩宣宣 张开来 王丹军 付峰(11)
- PdAu 合金泡沫膜的制备及其对乙醇的电催化活性(英文)
..... 刘军 周全 谢佳琦 李容(21)
- 热处理对富氮碳纳米纤维结构及储锂性能的影响
..... 王靖靖 张江 王金月 王璐 李轩科(31)
- 共沉淀法制备稀土 Ce 掺杂的纳米 ZnO 及其光催化降解染料的性能
..... 钟伟 夏颖帆 翟杭玲 高越 李世慧 吕春欣(40)
- 介孔 SBA-15 棒负载的 Pd_3Cl 催化剂催化 Sonogashira 偶联反应(英文)
..... 何蓉 负亚培 孙莉莉 盛鸿婷 杜袁鑫
项东 李鹏 袁孝友 朱满洲 洪勋 吴宇恩(53)
- $\text{Co}_3\text{V}_2\text{O}_9$ /石墨烯复合负极材料的合成及其储锂性能
..... 郑浩 金佳幸 程劲松 赵荣飞 李琳(62)
- 水热法合成 $\text{AgInS}_2/\text{ZnS}$ 核/壳结构量子点及其荧光性能
..... 陈婷 胡晓博 徐彦乔 王连军 江莞 江伟辉 谢志翔(69)
- 长寿命高镍无钴锂离子正极材料的制备
..... 班丽卿 柏祥涛 庄卫东 李文进 黄巍 卢世刚(79)
- 金属 Sr、Fe 掺杂对 LaCoO_3 催化氧化碳烟及抗硫性能影响
..... 魏炜 吴艾纯 乔智威 李树华 梁红 彭峰(87)
- 一种用于活体细胞 Zn^{2+} 检测的高灵敏度比例计量荧光探针
..... 张长丽 徐鉴 黄芳 赵海荣 陈昌云(97)
- 普鲁士蓝正极材料的离子交换法制备及电化学储钾性能
..... 孙云坡 谢健 赵新兵 庄大高 张根林(106)
- 化学-微波法制备高膨胀率膨胀蛭石及对亚甲基蓝的吸附机理
..... 解颜岩 孙红娟 彭同江 罗利明 田景斐 秦亚婷(113)
- 一种天线分子与卟啉染料自组装在染料敏化太阳能电池中的应用
..... 贾海浪 李珊珊 龚炳泉 顾磊 关明云(123)
- 不对称 Salen 配体的 $\text{Ni(II)}/\text{Cu(II)}/\text{Mn(III)}$ 配合物的合成及其晶体结构
..... 张奇龙 王家忠 杨小生 朱必学(132)
- 基于手性 MOF 与乙炔黑修饰电极对多巴胺和尿酸的同时检测(英文)
..... 方智利 王平 刘胜东 王欣 聂启祥 杨绍明 徐文媛 周枚花(139)

CF _x -Ru 复合阴极材料的制备及在锂一次电池中的应用(英文)	张伶俐 张丽娟 希利德格 李 钊	148
1,3-二(4-咪唑基)苯构筑的两个金属-有机框架化合物:合成、晶体结构和荧光性质(英文)	刘志强 武峻峰 陈 俊 吴 夏 王 彦	159
两个三维柱层式单一手性配位化合物:合成、结构和性质(英文)	徐中轩 柏雪累 蒙 琴	165
基于芳香四羧酸构筑的两种配位聚合物的荧光及磁性质(英文)	翟丽军 张 婕 高玲玲 高 婷 贾焦焦 牛宇岚 胡拖平	173
两个二亚胺-铜(I)-膦配合物的合成、结构和太赫兹时域光谱(英文)	朱 宁 潘 迅 林 森 杨玉平 辛秀兰 李中峰 张 帆 金琼花	183
一维镉(II)和镍(II)配位聚合物的合成、晶体结构、荧光及磁性质(英文)	黎 彧 陈泳璇 赵 娜 冯安生 邹训重	192
《无机化学学报》投稿须知		199

CHINESE JOURNAL OF INORGANIC CHEMISTRY

Vol.36

No.1

Jan. 2020

CONTENTS

Cover



Mesoporous SBA-15 Rods Supported Pd₃Cl Catalysts for Sonogashira C-C Coupling (English)

HE Rong, YUN Ya-Pei, SUN Li-Li, SHENG Hong-Ting, DU Yuan-Xin, XIANG Dong, LI Peng, YUAN Xiao-You, ZHU Man-Zhou, HONG Xun, WU Yu-En

DOI:10.11862/CJIC.2020.022

Chinese J. Inorg. Chem., 2020,36(1):53-61

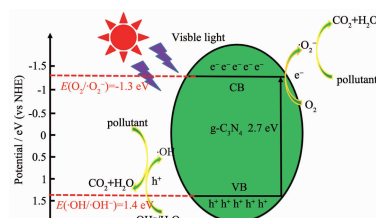
Articles

Effect of Nitric Acid Activation Melamine Precursor on Structure and Visible-Light Photocatalytic Performance of g-C₃N₄

YE Shi-Xiong, SHU Qing

DOI:10.11862/CJIC.2019.262

Chinese J. Inorg. Chem., 2020,36(1):1-10



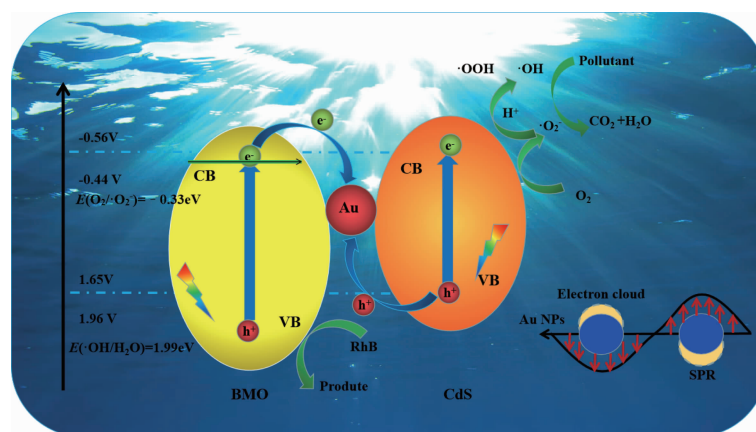
α -HNO₃-g-C₃N₄ which had high catalytic activity and stability was synthesized from the activation of melamine by HNO₃. A multilayered buildup structure was formed, which increased specific surface area and pores volume of sample. Consequently, the carrier transport capacity was significantly enhanced, and band gap dropped to 2.7 eV.

Design and Construction of All-Solid Z-Scheme CdS/Au/Bi₂MoO₆ Heterostructure with Enhanced Photocatalytic Performance

GUO Li, ZHAO Qiang, ZHANG Yue-Cheng, ZHANG Yuan-Yuan, HAN Xuan-Xuan, ZHANG Kai-Lai, WANG Dan-Jun, FU Feng

DOI:10.11862/CJIC.2020.023

Chinese J. Inorg. Chem., 2020,36(1):11-20



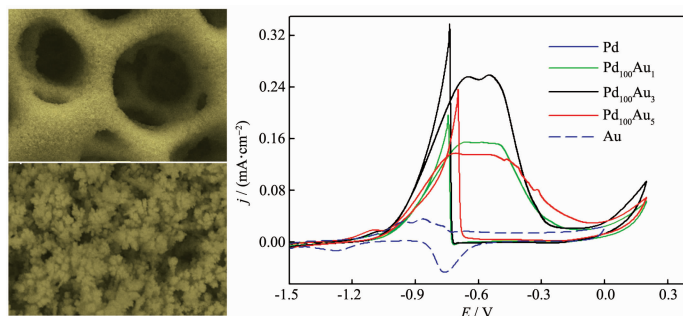
Z-scheme CdS/Au/Bi₂MoO₆ heterostructure have been successfully fabricated by co-modification with CdS and Au on the surface of Bi₂MoO₆, thus significantly improving photocatalytic activity of Bi₂MoO₆.

Preparation and High Electrocatalytic Activity for the Oxidation of Ethanol of PdAu Alloy Foam Films (English)

LIU Jun, ZHOU Quan, XIE Jia-Qi, LI Rong

DOI:10.11862/CJIC.2019.195

Chinese J. Inorg. Chem., 2020,36(1):21-30



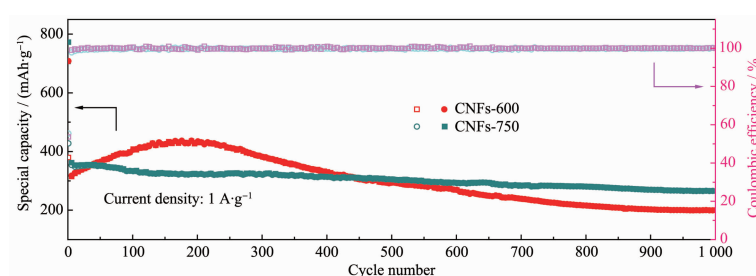
Three-dimensional (3D) porous Au-doped PdAu alloy foam films were obtained by using a hydrogen bubble dynamic template electrodeposition method. The Au-doped PdAu alloy foam films showed high electrocatalytic activity toward the electrooxidation of ethanol in alkaline media.

Effect of Heat Treatment on Structure and Lithium Ion Storage Properties of N-Rich Carbon Nanofibers

WANG Jing-Jing, ZAHNG Jiang, WANG Jin-Yue, WANG Lu, LI Xuan-Ke

DOI:10.11862/CJIC.2020.026

Chinese J. Inorg. Chem., 2020,36(1):31-39



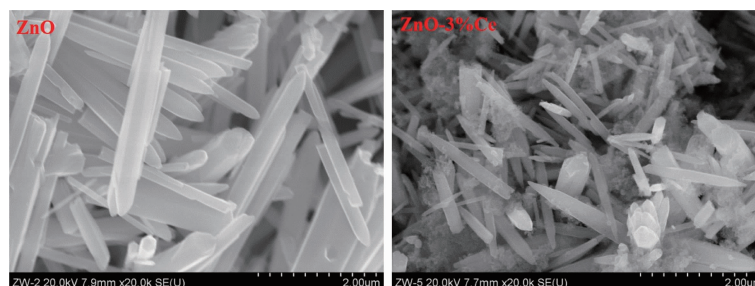
The type and content of nitrogen in CNFs prepared at different carbonization temperature can improve the storage performance of Li⁺ in LIBs, and then improve the capacity of electrode.

Preparation by Co-precipitation Method and Photocatalytic Performances on the Degradation of Dyes of Ce³⁺-Doped Nano-ZnO

ZHONG Wei, XIA Ying-Fan, ZHAI Hang-Ling, GAO Yue, LI Shi-Hui, LÜ Chun-Xin

DOI:10.11862/CJIC.2020.006

Chinese J. Inorg. Chem., 2020,36(1):40-52



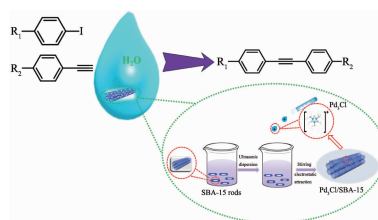
Moderate doping of Ce³⁺ can change the morphology of nano-ZnO and greatly improve the photocatalytic degradation activity of organic dyes

Mesoporous SBA-15 Rods Supported Pd₃Cl Catalysts for Sonogashira C-C Coupling (English)

HE Rong, YUN Ya-Pei, SUN Li-Li, SHENG Hong-Ting, DU Yuan-Xin, XIANG Dong, LI Peng, YUAN Xiao-You, ZHU Man-Zhou, HONG Xun, WU Yu-En

DOI:10.11862/CJIC.2020.022

Chinese J. Inorg. Chem., 2020,36(1):53-61



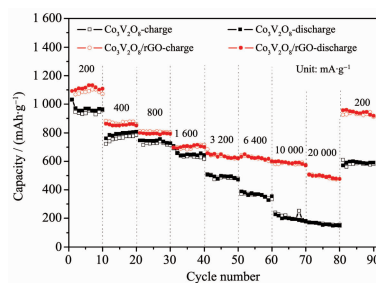
Atomically precise [Pd₃Cl(PPh₂)₂(PPh₃)₃]⁺ (denoted as Pd₃Cl) nanoclusters were supported on mesoporous SBA-15 by electrostatic attraction strategy. The well-defined Pd₃Cl/SBA-15 catalysts exhibited high catalytic activities and good recyclability for Sonogashira C-C coupling reaction.

Preparation and Electrochemical Properties of $\text{Co}_3\text{V}_2\text{O}_8/\text{graphene}$ Composite of Anode Material for Lithium Storage

ZHENG Hao, JIN Jia-Xin, CHENG Jing-Song, ZHAO Rong-Fei, LI Lin

DOI:10.11862/CJIC.2020.010

Chinese J. Inorg. Chem., **2020**,**36**(1):62-68



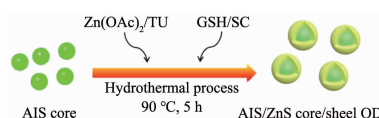
The $\text{Co}_3\text{V}_2\text{O}_8/\text{rGO}$ composite has been successfully prepared by through a facile hydrothermal combined thermal treatment method. The excellent electrochemical performance is attributed to the synergistic effect from reduced graphene oxide and $\text{Co}_3\text{V}_2\text{O}_8$, and the composite structure can improve the electrode conductivity and efficient buffering the volume change.

Hydrothermal Synthesis and Fluorescence Properties of $\text{AgInS}_2/\text{ZnS}$ Core/Shell Quantum Dots

CHEN Ting, HU Xiao-Bo, XU Yan-Qiao, WANG Lian-Jun, JIANG Wan, JIANG Wei-Hui, XIE Zhi-Xiang

DOI:10.11862/CJIC.2020.024

Chinese J. Inorg. Chem., **2020**,**36**(1):69-78



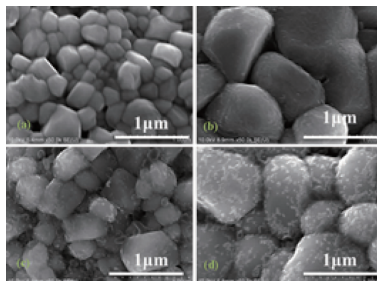
AIS/ZnS core/shell QDs with high crystallinity and stability were synthesized via hydrothermal method with adding ZnS precursors into AIS cores solution. In contrast with AIS QDs, the AIS/ZnS core/shell QDs show significantly improved emissive intensity, which increases with increasing the reaction temperature and the addition amount of ligands.

Preparation of Long-Life Nickel-Rich and Cobalt-Free Layered $\text{LiNi}_{0.75}\text{Mn}_{0.25}\text{O}_2$ Cathode Materials

BAN Li-Qing, BAI Xiang-Tao, ZHUANG Wei-Dong, LI Wen-Jin, HUANG Wei, LU Shi-Gang

DOI:10.11862/CJIC.2020.011

Chinese J. Inorg. Chem., **2020**,**36**(1):79-86



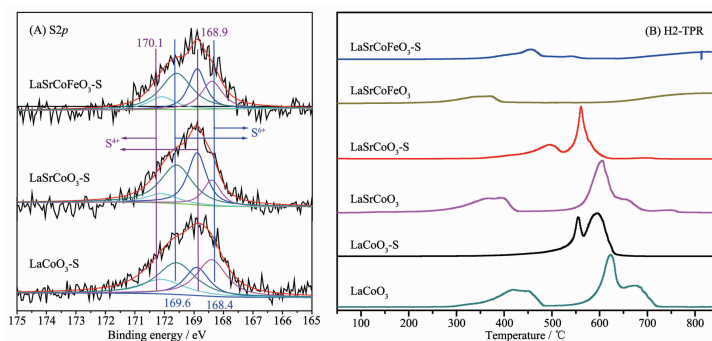
The $\text{LiNi}_{0.75}\text{Mn}_{0.25}\text{O}_2$ material exhibited a low residual alkali content and a high cyclability, with 80% capacity retention after 830 cycles under the coating modification with a mechanical fusion method.

Effect of Sr and Fe Doped LaCoO_3 on Catalytic Oxidation of Soot and Sulfur Resistance

WEI Wei, WU Ai-Chun, QIAO Zhi-Wei, LI Shu-Hua, LIANG Hong, PENG Feng

DOI:10.11862/CJIC.2020.031

Chinese J. Inorg. Chem., **2020**,**36**(1):87-96



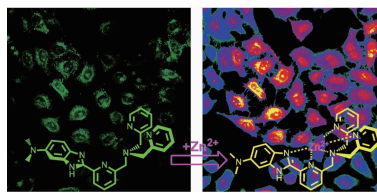
The catalysts exhibited excellent catalytic oxidation soot activity and sulfur resistance. Moreover, the poisoning of SO_2 was mainly attributed to the sulfation (SO_3^{2-} , SO_4^{2-}) of $\text{Co}^{2+}/\text{Co}^{3+}$ and surface adsorbed oxygen, leading to deactivating the active site (O_2^- or O^- and Fe^{4+}) of catalyst.

A Highly Sensitive Ratiometric
Fluorescence Probe for Zn^{2+} Detection in
Living Cells

ZHANG Chang-Li, XU Jian, HUANG Fang,
ZHAO Hai-Rong, CHEN Chang-Yun

DOI:10.11862/CJIC.2020.009

Chinese J. Inorg. Chem., 2020,36(1):97-105



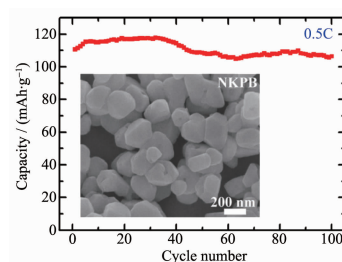
A ratiometric fluorescent Zn^{2+} sensor **DBITA** which featured a Zn^{2+} -induced large Stokes shift of 172 nm and picomolar sensitivity for Zn^{2+} detection in both aqueous media and living cells was developed.

Prussian Blue Cathode Material:
Preparation by Ion-Exchange Method and
Electrochemical Potassium-Storage
Performance

SUN Yun-Po, XIE Jian, ZHAO Xin-Bing,
ZHUANG Da-Gao, ZHANG Gen-Lin

DOI:10.11862/CJIC.2020.008

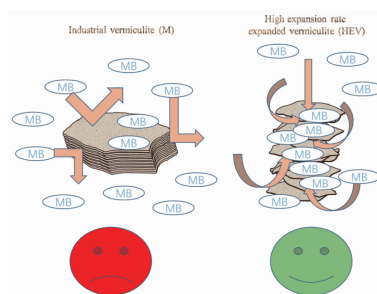
Chinese J. Inorg. Chem., 2020,36(1):106-112



A Na-doped K-based Prussian blue material $K_{1.9}Na_{0.1}Mn[Fe(CN)_6] \cdot 0.4H_2O$ prepared by an ion-exchange method showed a high capacity of $136.3 \text{ mAh} \cdot \text{g}^{-1}$ at 0.1C, good rate capability of $68.4 \text{ mAh} \cdot \text{g}^{-1}$ at 10C and good cycling stability with 96.1% capacity retained after 100 cycle at 0.5C.

High Expansion Rate Expanded
Vermiculite: Preparation by
Chemical-Microwave Method and the
Adsorption Mechanism of Methylene Blue

XIE Yan-Yan, SUN Hong-Juan,
PENG Tong-Jiang, LUO Li-Ming, TIAN Jing-Fei,
QIN Ya-Ting



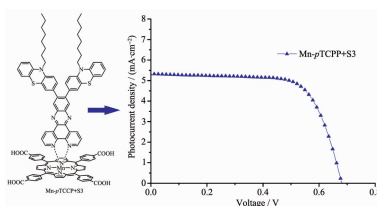
To improve vermiculite application efficiency and broaden its application field, we prepared HEV and tested its adsorption effect on MB. The results showed that the MB adsorption capacity of HEV was higher than that of some natural clay minerals and commercial grade activated carbon.

DOI:10.11862/CJIC.2020.004

Chinese J. Inorg. Chem., 2020,36(1):113-122

Application of Self-Assembly of an
Antenna Molecule with Porphyrin Dyes in
Dye-Sensitized Solar Cells

JIA Hai-Lang, LI Shan-Shan, GONG Bing-Quan,
GU Lei, GUAN Ming-Yun



The antenna molecule S3 effectively enhances the spectral responsiveness of the DSSC, making the conversion efficiency increase by 1.2 times.

DOI:10.11862/CJIC.2020.014

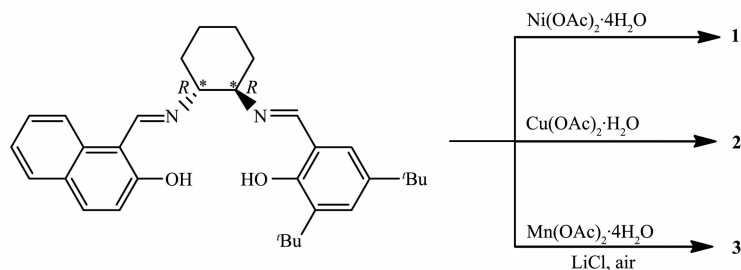
Chinese J. Inorg. Chem., 2020,36(1):123-131

Synthesis and Crystal Structure of Ni(II)/
Cu(II)/Mn(III) Complexes with Asymmetric
Salen Ligand

ZHANG Qi-Long, WANG Jia-Zhong,
YANG Xiao-Sheng, ZHU Bi-Xue

DOI:10.11862/CJIC.2020.030

Chinese J. Inorg. Chem., **2020**,**36**(1):132-138

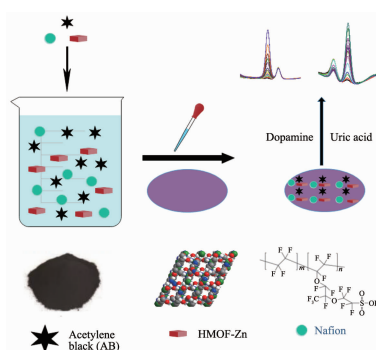


Simultaneous Detection of Dopamine and
Uric Acid Based on Chiral MOF and
Acetylene Black Modified Electrode
(English)

FANG Zhi-Li, WANG Ping, LIU Sheng-Dong,
WANG Xin, NIE Qi-Xiang, YANG Shao-Ming,
XU Wen-Yuan, ZHOU Mei-Hua

DOI:10.11862/CJIC.2019.273

Chinese J. Inorg. Chem., **2020**,**36**(1):139-147



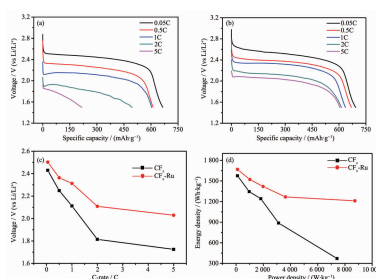
The GCE electrode modified by a kind of chiral MOF blended with acetylene black that fixed by Nafion had a high electrical signal response to dopamine and uric acid. Dopamine and uric acid can be simultaneously detected on the modified GCE electrode and totally independent of each other.

CF_x-Ru Composite Cathode for Lithium
Primary Battery with Significantly
Improved Electrochemical Performance
(English)

ZHANG Ling-Xiao, ZHANG Li-Juan,
XILI De-Ge, LI Fan

DOI:10.11862/CJIC.2020.005

Chinese J. Inorg. Chem., **2020**,**36**(1):148-158



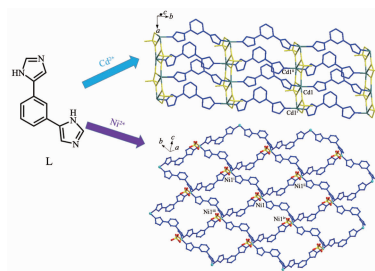
The ruthenium-modified fluorocarbons as anode material of lithium primary battery showed excellent rate capability and energy density, which is attributed to the removal of inert groups and the increase of specific surface area during the introduction of ruthenium.

Two Metal-Organic Frameworks
Constructed by 1,3-Di(1*H*-imidazol-4-yl)
Ligand: Synthesis, Crystal Structure and
Photoluminescence Property (English)

LIU Zhi-Qiang, WU Jun-Feng, CHEN Jun,
WU Xia, WANG Yan

DOI:10.11862/CJIC.2020.003

Chinese J. Inorg. Chem., **2020**,**36**(1):159-164



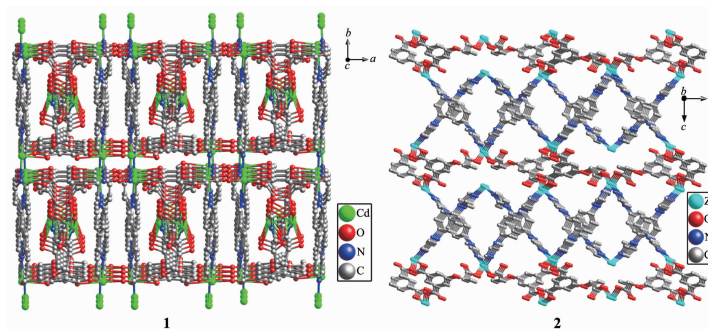
Two complexes, [Cd(L)(SO₄)]_n (**1**) and {[Ni(L)(SO₄)]·H₂O}_n (**2**) (L=1,3-di(1*H*-imidazol-4-yl)benzene) were structurally characterized, and their thermal stability and luminescent properties were presented.

Two 3D Pillar-Layered Homochiral Coordination Complexes: Syntheses, Structures and Properties (English)

XU Zhong-Xuan, BAI Xue-Lei, MENG Qin

DOI:10.11862/CJIC.2020.029

Chinese J. Inorg. Chem., **2020**,**36**(1):165-172

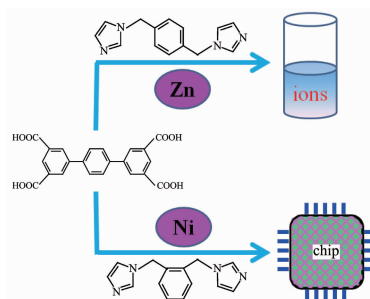


Two Coordination Polymers Constructed by Aromatic Tetracarboxylic Acid: Luminescent and Magnetic Properties (English)

ZHAI Li-Jun, ZHANG Jie, GAO Ling-Ling, GAO Ting, JIA Jiao-Jiao, NIU Yu-Lan, HU Tuo-Ping

DOI:10.11862/CJIC.2019.257

Chinese J. Inorg. Chem., **2020**,**36**(1):173-182



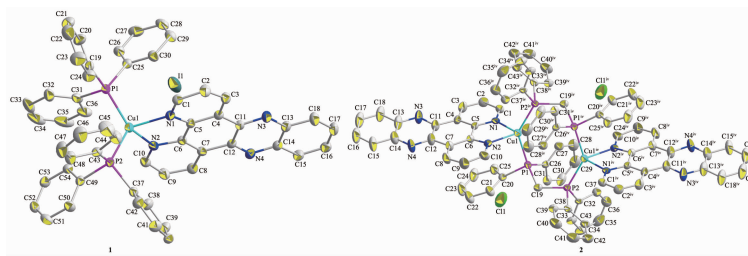
Complex **1** is good luminescent probe for detecting $\text{Fe}^{3+}/\text{Cr}_2\text{O}_7^{2-}$ and complex **2** shows antiferromagnetic properties.

Syntheses, Structures and Terahertz Time-Domain Spectroscopy of Two Diimine-Copper(I)-Phosphine Complexes (English)

ZHU Ning, PAN Xun, LIN Sen, YANG Yu-Ping, XIN Xiu-Lan, LI Zhong-Feng, ZHANG Fan, JIN Qiong-Hua

DOI:10.11862/CJIC.2020.015

Chinese J. Inorg. Chem., **2020**,**36**(1):183-191



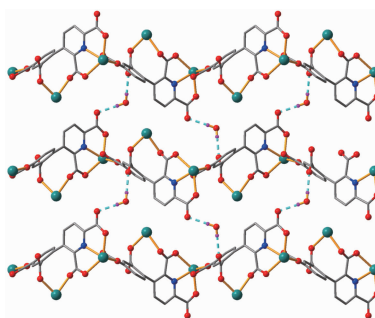
Complex **1** is of simple mononuclear structure. Complex **2** is different from **1** for its dinuclear geometry structure because of the phosphine ligand dppm replacing PPh_3 . The room temperature terahertz (THz) absorption spectra of complexes **1-2** provides useful information for the properties of complexes.

Syntheses, Crystal Structures, Luminescent and Magnetic Properties of Two 1D Cadmium(II) and Nickel(II) Coordination Polymers (English)

LI Yu, CHEN Yong-Xuan, ZHAO Na, FENG An-Sheng, ZOU Xun-Zhong

DOI:10.11862/CJIC.2020.017

Chinese J. Inorg. Chem., **2020**,**36**(1):192-198



Two 1D chain $\{[\text{M}_2(\mu_3\text{-L})(\text{phen})_3] \cdot 5\text{H}_2\text{O}\}_n$ ($\text{M}=\text{Cd}$ (**1**), Ni (**2**)) have been constructed and the structures, luminescent and magnetic properties of the polymers were investigated.